

Analysis and efficient solution of stationary Schrödinger equation governing electronic states of quantum dots and rings in magnetic field

Marta M. Betcke ^{*} Heinrich Voss [†]

January 15, 2010

Abstract

In this work the one-band effective Hamiltonian governing the electronic states of a quantum dot/ring in a homogenous magnetic field is used to derive a pair/quadruple of nonlinear eigenvalue problems corresponding to different spin orientations and in case of rotational symmetry additionally to quantum number $\pm\ell$. We show, that each of those pair/quadruple of nonlinear problems allows for the minmax characterization of its eigenvalues under certain conditions, which are satisfied for our examples and the common InAs/GaAs heterojunction. Exploiting the minmax property we devise efficient iterative projection methods simultaneously handling the pair/quadruple of nonlinear problems and thereby saving up to 40% of the computational time as compared to the Nonlinear Arnoldi method applied to each of the problems separately.

Keywords: Quantum dot, quantum ring, nonlinear eigenvalue problem, minmax characterization, iterative projection method, electronic state, spin orbit interaction, magnetic field

AMS Subject Classification: 65F15, 65F50

1 Introduction

The spectroscopic techniques involving magnetic field have for long been employed in experimental studies of bulk materials. However, only recently, methods like resonant spin-flip Raman scattering have been applied to quantum dots [22]. The analysis of Zeeman levels and the associated Landé factors allows the

^{*}Department of Computer Science, University College London, Gower Street, London WC1E 6BT, UK, m.betcke@cs.ucl.ac.uk

[†]Institute of Numerical Simulation, Hamburg University of Technology, D-21071 Hamburg, Germany, voss@tu-harburg.de

physicists for better understanding of spin effects on the optical response of low dimensional systems and is crucial for interpretation of the results of spectroscopic analysis, magneto-optical experiments or magneto-transport phenomena.

Over the last four decades the density of transistors in integrated circuits has been exponentially growing (Moore's law). Nowadays we have devices of size well below 100nm and we are fast approaching the limit of what is possible with the presently available manufacturing technologies. As a result increasing efforts are being directed to development of novel technologies like for instance nanoscale electronic devices utilizing the effect of spin polarization along with the electronic charge. Such devices could replace the widely used CMOS technology and are potential candidates for the implementation of quantum computers. Since the successful application of the magnetic field to manipulate the spin polarization in the semiconductors resulting in market ready devices like spin valve, semiconductor nanostructures are in focus of research on magneto-electronics. In semiconductor nanostructures the free carriers are confined to a small region of space by the potential barriers. Moreover, if the size of this region is less than the electron wavelength, the electronic states become quantized at discrete energy levels. The ultimate limit of such low dimensional structures is the quantum dot, in which the free carriers are confined in all three directions of space. Such an energy quantization is an intrinsic property of an atom, which makes the quantum dot also an interesting model for investigation of properties of systems at atomic level. These and many others applications show the importance of examining the influence of the magnetic field on the electronic levels of the semiconductor nanostructures.

In this work we consider the Zeeman splitting of energy levels of quantum dots and rings in an external homogenous magnetic field. The internal Zeeman effect i.e. the splitting of electronic levels due to the interaction of the spin magnetic moment with the magnetic field acting on the electron while precessing around the nucleus, was considered in [5]. We discuss the general three dimensional case on an example of a pyramidal quantum dot and the rotationally symmetric case on an example of an elliptical quantum ring. We assume the one-band Hamiltonian with nonparabolic effective mass approximation and the effective Landé factor for the electronic states in the conduction band. This model yields a magnetic stationary Schrödinger equation, where the eigenvalue parameter enters nonlinearly. Considering different spin orientations we obtain a pair of nonlinear eigenvalue problems, one for each spin orientation. In case of rotational symmetry additionally the combination of the $\pm\ell$ quantum numbers leads to four different nonlinear eigenvalue problems. We derive sufficient conditions for the physically relevant eigenvalues of the corresponding variational problems to satisfy the minmax principle [30]. These conditions hold for the InAs/GaAs heterojunctions in our examples. Exploiting the minmax property we develop efficient iterative projection methods which simultaneously handle the pair/quadruple of the nonlinear problems considerably reducing the overall computational time.

Our paper is organized as follows. In Section 2 we introduce the magnetic one-band effective Hamiltonian which models the electronic behavior of the three

dimensional quantum structures. The derivation of the corresponding pair of rational eigenvalue problems and their analysis is provided in Section 3. In Section 4 we adapt the model to a nano-ring in magnetic field. Further, we derive the corresponding quadruple of nonlinear eigenvalue problems and analyze it. In Section 5 we give the minmax characterization for both problems and their discretizations obtained with Galerkin methods. The resulting rational matrix eigenvalue problems are large and sparse and therefore they can be efficiently handled by iterative projection methods like e.g. Jacobi Davidson [7] or Non-linear Arnoldi [26], which are briefly recalled in Section 6. In Section 7 we describe modifications of the iterative projection methods tailored to simultaneously handle the pair/quadruple of the nonlinear eigenvalue problems thereby saving considerable amount of the computational time. We demonstrate the efficiency of our methods on numerical examples. The conclusions together with some ideas for future research are summarized in the last section.

2 One-band effective Hamiltonian in magnetic field

We consider the magnetic one-band effective Hamiltonian for electrons in the conduction band [3, 8]

$$H = (-i\hbar\nabla + eA) \frac{1}{2m(\lambda, x)} (-i\hbar\nabla + eA) + V(x) + \mu_B \frac{g(\lambda, x)}{2} \sigma B, \quad (1)$$

where \hbar is the reduced Planck constant, ∇ denotes the spatial gradient and $A(x)$ the vector potential such that $B = \nabla \times A(x)$ is the magnetic field intensity. Further, e and m_0 are the free electron charge and mass, $\mu_B = \frac{e\hbar}{2m_0}$ is the Bohr magneton and σ is the vector of Pauli matrices.

Assuming nonparabolicity for the electron's dispersion relation, the electron effective mass $m(\lambda, x)$ is constant on the dot $\Omega_q \subset \mathbb{R}^3$ and on the surrounding matrix $\Omega_m \subset \mathbb{R}^3$ for every fixed energy level λ , and is taken as [3, 8]

$$\frac{1}{m_j(\lambda)} := \frac{1}{m(\lambda, x)} \Big|_{x \in \Omega_j} = \frac{P_j^2}{\hbar^2} \left(\frac{2}{\lambda + E_{g,j} - V_j} + \frac{1}{\lambda + E_{g,j} - V_j + \Delta_j} \right),$$

for $j \in \{q, m\}$. Here the confinement potential $V_j := V|_{\Omega_j}$ is piecewise constant, and P_j , $E_{g,j}$ and Δ_j are the momentum matrix element, the band gap, and the spinorbit splitting in the valence band for the quantum dot material ($j = q$) and the matrix ($j = m$), respectively. The values of the semiconductor parameters are depicted in Table 1. It is known that pyramid shape dots are under significant degree of strain, which in turn affects the electronic levels of the quantum dot. Therefore for simulations with pyramidal shapes we adapted the strain model used in [6] resulting in strained values of the band gap E_p and the confinement potential V .

Table 1: Semiconductor parameters, values without and with strain.

	P	Δ	E_g	V	strained E_g	strained V
InAs	0.7509	0.48	0.42	0	0.943	0
GaAs	0.7848	0.34	1.52	0.77	1.52	0.395

The effective Landé factor $g(\lambda, x)$ in equation (1) is given by the following equation [3]

$$g_j(\lambda) := g(\lambda, x)|_{x \in \Omega_j} = 2 \left\{ 1 - \frac{m_0}{m_j(\lambda)} \frac{\Delta_j}{3(\lambda + E_{g,j} - V_j) + 2\Delta_j} \right\}, \quad j \in \{q, m\}.$$

Analogously to the effective mass, for a fixed energy level λ , $g(\lambda, x)$ is a piecewise constant function.

The energy states and corresponding wave functions for electrons are obtained from the Schrödinger equation

$$\frac{1}{2m_j(\lambda)} (-i\hbar\nabla + eA(x))^2\Phi + V_j\Phi + \mu_B \frac{g_j(\lambda)}{2} \sigma B\Phi = \lambda\Phi, \quad j \in \{q, m\}, \quad (2)$$

and for physical applications the interesting eigenvalues are those in the interval (V_q, V_b) , which are the discrete part of the spectrum of the Hamiltonian (1) for the unbounded domain Ω_m . These eigenvalues are also called confined states, since the corresponding wave functions Φ live mainly on the quantum structure and decay rapidly outside of the structure. For this reason it is appropriate to consider the eigenvalue problem on a bounded matrix domain Ω_m with homogenous Dirichlet conditions on the outer boundary of the matrix.

We assume a constant magnetic field $B = (0, 0, B)$ perpendicular to the (x, y) -plane, and we choose the symmetric gauge $A(x, y, z) = \frac{1}{2}(-y, x, 0) \in C^\infty(\mathbb{R}^3, \mathbb{R}^3)$. We do not explicitly distinguish between the vector of the magnetic field intensity and its z th component, but the meaning will be clear from the context. On the interface between the dot and the matrix the electron wave functions are continuous and since $A(x) \in C^\infty(\mathbb{R}^3, \mathbb{R}^3)$ the Ben Daniel-Duke condition is appropriate [3, 25]

$$\frac{1}{m_q(\lambda)} \frac{\partial\Phi(x)}{\partial\bar{n}_q} = \frac{1}{m_m(\lambda)} \frac{\partial\Phi(x)}{\partial\bar{n}_m}, \quad x \in \partial\Omega_{int},$$

where $\partial\Omega_{int} = \partial\Omega_q \cap \partial\Omega_m$ and \bar{n}_q, \bar{n}_m denote the outward normal vector of the dot and the matrix, respectively.

In this work we focus on two models: a fully three dimensional quantum dot model and an axially symmetric quantum ring model. The fully three dimensional case is considered in Section 3. The second model allows for the separation of the angular direction hence resulting in equation with a different structure which is handled separately in Section 4. We would like to point

out that the ideas presented in this work can also be applied to more general structures in particular to quantum dots on wetting layers and to arrays of quantum dots with or without the axial symmetry.

3 Quantum dot in magnetic field

First, we consider a quantum dot $\Omega_q \subset \mathbb{R}^3$ embedded into a cuboid matrix $\Omega_m \subset \mathbb{R}^3$, which is exposed to a homogenous magnetic field (cf. Figure 1).

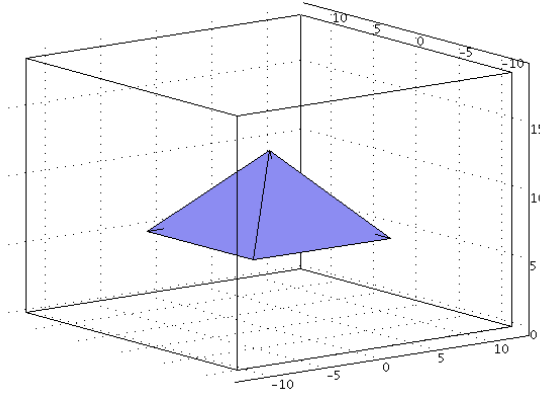


Figure 1: Pyramidal quantum dot embedded in a cuboid matrix.

We recall that the eigenvalues of the physical relevance are those not exceeding the confinement potential. Therefore, for the sake of simplicity we gage the potential $V_q = 0$, so that the relevant eigenvalues are in the interval $J := (0, V_m)$. In this section we derive the characterization of these eigenvalues as the minmax values of a Rayleigh functional.

Let $\Omega := \bar{\Omega}_q \cup \Omega_m$. An appropriate space for the magnetic Schrödinger operator with the vector potential A is (cf. [9, 15])

$$H_A^1(\Omega) := \{ \phi : \Omega \rightarrow \mathbb{C} : \phi \in L^2(\Omega) \text{ and } (\nabla + iA)\phi \in L^2(\Omega) \}$$

and the associated inner product is

$$\langle \phi, \psi \rangle_{H_A} := \int_{\Omega} \phi \bar{\psi} dx + \int_{\Omega} (\nabla + iA)\phi \cdot \overline{(\nabla + iA)\psi} dx. \quad (3)$$

Due to the continuity of A and since Ω is bounded with Lipschitz boundary it can be shown that $\phi \in H_A^1(\Omega)$ if and only if $\phi \in H^1(\Omega)$, and there exist $c_1, c_2 > 0$ such that

$$c_1 \|\phi\|_{H^1(\Omega)} \leq \|\phi\|_{H_A^1(\Omega)} \leq c_2 \|\phi\|_{H^1(\Omega)} \quad \text{for all } \phi \in H^1(\Omega),$$

where $\|\cdot\|_{H_A^1(\Omega)}$ denotes the norm induced by (3) (cf. [1, 4]).

To account for the Dirichlet boundary conditions on the exterior of the matrix we define the trial function space

$$H := \{ \phi \in H_{\tilde{A}}^1 : \phi(x) = 0, \quad x \in \partial\Omega \},$$

where $\partial\Omega = \partial\Omega_m \setminus \partial\Omega_{int}$ is the outer boundary of the structure and the vector potential has been rescaled according to (1), $\tilde{A}(x) = \frac{\epsilon}{\hbar} A(x)$. We choose on H the norm induced by the quadratic form associated with the magnetic Schrödinger operator

$$\|\phi\|_H := \left(\int_{\Omega} |\nabla\phi + i\tilde{A}\phi|^2 dx \right)^{1/2}.$$

By virtue of the diamagnetic inequality [15]

$$|\nabla|\phi|(x)| \leq |(\nabla + i\tilde{A})\phi(x)| \quad \text{for all } \phi \in H_{\tilde{A}}^1(\Omega) \text{ and a.e. } x \in \Omega$$

and Friedrich's inequality for $\nabla|\phi|$, this is equivalent to the scalar product induced norm on $H_{\tilde{A}}^1$ and therewith to $\|\phi\|_{H_0^1(\Omega)} := \|\nabla\phi\|_{L^2(\Omega)}$. Therefore $H(\Omega)$ is compactly embedded in $L^2(\Omega)$ along with $H^1(\Omega)$. The details of the argument are given in [4].

Now, we are in the position to set up the variational form of the Schrödinger equation. Multiplying (2) with $\bar{\psi}$ and integrating over Ω we arrive at

$$\begin{aligned} a_{\pm}(\phi, \psi; \lambda) &:= \frac{\hbar^2}{2m_q(\lambda)} \int_{\Omega_q} (\nabla + i\tilde{A})\phi \cdot \overline{(\nabla + i\tilde{A})\psi} dx \\ &+ \frac{\hbar^2}{2m_m(\lambda)} \int_{\Omega_m} (\nabla + i\tilde{A})\phi \cdot \overline{(\nabla + i\tilde{A})\psi} dx + V_m \int_{\Omega_m} \phi \bar{\psi} dx \\ &\pm \left(\gamma_q^B(\lambda) \int_{\Omega_q} \phi \bar{\psi} dx + \gamma_m^B(\lambda) \int_{\Omega_m} \phi \bar{\psi} dx \right) \\ &= \lambda \int_{\Omega} \phi \bar{\psi} dx =: \lambda b(\phi, \psi) \quad \text{for every } \psi \in H, \end{aligned} \quad (4)$$

where $\gamma_j^B(\lambda) = \frac{1}{2} \mu_B B g_j(\lambda)$.

The quadratic form $b(\cdot, \cdot)$ obviously is sesquilinear, positive, and bounded on $L^2(\Omega)$.

Under the assumption $E_{g,j} - V_j > 0$ the functions $\lambda \mapsto \frac{1}{m_j(\lambda)}$ are defined for $\lambda \geq 0$, and are positive and monotonically decreasing. Moreover, $g_j(\lambda)$ and therewith $\gamma_j^B(\lambda)$ are monotonically increasing for $B > 0$ and bounded on J . Hence $a_{\pm}(\cdot, \cdot; \lambda)$ is a symmetric sesquilinear form and since $(\nabla + i\tilde{A})\phi \in L^2(\Omega)$ by virtue of the Hölder inequality

$$\left| \int_{\Omega} (\nabla + i\tilde{A})\phi \cdot \overline{(\nabla + i\tilde{A})\psi} dx \right| \leq \|(\nabla + i\tilde{A})\phi\| \|(\nabla + i\tilde{A})\psi\|,$$

and therefore by the embedding of $H \hookrightarrow L^2$, $a_{\pm}(\cdot, \cdot; \lambda)$ is bounded on H .

If $B = 0$, i.e. in the absence of the magnetic field, $\gamma_j^B(\lambda) = 0$ for $j = \{q, m\}$ and there is no level splitting. Problems of this type were investigated in [4, 6, 17, 29] and the minmax characterization is given therein.

For $B \neq 0$ the ellipticity can not be argued unconditionally as in the case $B = 0$. The following lemma contains a sufficient condition for $a_{\pm}(\cdot, \cdot; \lambda)$ to be H -elliptic for all $\lambda \in J$ such that each of the linear eigenvalue problems

$$\text{Find } \mu^{\pm} \text{ and } \phi \in H, \phi \neq 0 \text{ with } a_{\pm}(\phi, \psi; \lambda) = \mu^{\pm} b(\phi, \psi) \quad \text{for every } \psi \in H \quad (5)$$

has a countable set of eigenvalues $0 < \mu_1^{\pm}(\lambda) \leq \mu_2^{\pm}(\lambda) \leq \dots$ which can be characterized by the minmax principle of Poincaré

$$\mu_j^{\pm}(\lambda) = \min_{\dim V=j, V \subset H} \max_{\phi \in V, \phi \neq 0} \frac{a_{\pm}(\phi, \phi; \lambda)}{b(\phi, \phi)}.$$

Lemma 3.1 *Let κ_{\min} be the smallest eigenvalue of the following linear eigenvalue problem*

$$c(\phi, \psi) := \int_{\Omega} (\nabla + i\tilde{A})\phi \cdot \overline{(\nabla + i\tilde{A})\psi} dx = \kappa \int_{\Omega} \phi \bar{\psi} dx \quad \text{for every } \psi \in H. \quad (6)$$

If

$$\min \left\{ \frac{\hbar^2}{2m_q(\lambda)}, \frac{\hbar^2}{2m_m(\lambda)} \right\} > \frac{\max\{|\gamma_q^B(\lambda)|, |\gamma_m^B(\lambda)| - V_m\}}{\kappa_{\min}} \quad \text{for every } \lambda \in J, \quad (7)$$

then $a_{\pm}(\cdot, \cdot; \lambda)$ is H -elliptic for every fixed $\lambda \in J$.

Proof: For $\phi \in H$ it holds that

$$\begin{aligned} a_{\pm}(\phi, \phi; \lambda) &\geq \min \left\{ \frac{\hbar^2}{2m_q(\lambda)}, \frac{\hbar^2}{2m_m(\lambda)} \right\} c(\phi, \phi) - \max\{|\gamma_q^B(\lambda)|, |\gamma_m^B(\lambda)| - V_m\} \int_{\Omega} |\phi|^2 dx \\ &\geq \left(\min \left\{ \frac{\hbar^2}{2m_q(\lambda)}, \frac{\hbar^2}{2m_m(\lambda)} \right\} - \frac{\max\{|\gamma_q^B(\lambda)|, |\gamma_m^B(\lambda)| - V_m\}}{\kappa_{\min}} \right) c(\phi, \phi) \\ &= \left(\min \left\{ \frac{\hbar^2}{2m_q(\lambda)}, \frac{\hbar^2}{2m_m(\lambda)} \right\} - \frac{\max\{|\gamma_q^B(\lambda)|, |\gamma_m^B(\lambda)| - V_m\}}{\kappa_{\min}} \right) \|\phi\|_H^2. \end{aligned}$$

We remark that for $B = 0$ the right hand side of (7) becomes 0 and since $\frac{\hbar^2}{2m_j(\lambda)} > 0$, $j \in \{q, m\}$ the condition is trivially satisfied, which is consistent with the earlier results in [4, 6, 17, 29]. \blacksquare

The variational characterizations for a linear eigenproblem $a(\phi, \psi) = \lambda b(\phi, \psi)$ employ the Rayleigh quotient $R(\phi) := a(\phi, \phi)/b(\phi, \phi)$ which is the unique solution of the real equation $f(\lambda; \phi) = \lambda b(\phi, \phi) - a(\phi, \phi)$. More generally, a variational characterization of real eigenvalues of a nonlinear eigenvalue problem

like (4) requires a Rayleigh functional, which is defined as a solution of the corresponding equation

$$f_{\pm}(\lambda; \phi) := \lambda b(\phi, \phi) - a_{\pm}(\phi, \phi; \lambda) = 0. \quad (8)$$

The following lemma contains a sufficient condition for the existence of such a Rayleigh functional.

Lemma 3.2 *Assume that the conditions of Lemma 3.1 hold, and*

$$-\frac{\hbar^2}{2} \max \left\{ \left(\frac{1}{m_q(\lambda)} \right)', \left(\frac{1}{m_m(\lambda)} \right)' \right\} > \frac{\max\{|\gamma_q'^B(\lambda)|, |\gamma_m'^B(\lambda)|\} - 1}{\kappa_{\min}} \quad \text{for every } \lambda \in J, \quad (9)$$

where κ_{\min} denotes the smallest eigenvalue of the eigenvalue problem (6).

Then for every $\phi \in H$, $\phi \neq 0$ each of the real equations f_{\pm} satisfies

$$f_{\pm}(0; \phi) < 0 \quad \text{and} \quad \frac{\partial}{\partial \lambda} f_{\pm}(\lambda; \phi) > 0 \quad \text{for every } \lambda \in J.$$

Hence, equation (8) implicitly defines a Rayleigh functional $p_{\pm} : H \supset D_{\pm} \rightarrow J$ for each of the eigenproblems (4) where $D_{\pm} := \{\phi \in H : f_{\pm}(\lambda; \phi) = 0 \text{ solvable in } J\}$.

Proof: $f_{\pm}(0; \phi) = -a_{\pm}(\phi, \phi; 0) < 0$ follows immediately from the ellipticity of $a_{\pm}(\cdot, \cdot; 0)$.

For every $\phi \in H$, $\phi \neq 0$ and every $\lambda \in J$ it holds that

$$\begin{aligned} \frac{\partial}{\partial \lambda} f_{\pm}(\lambda; \phi) &= - \left(\frac{\hbar^2}{2m_q(\lambda)} \right)' \int_{\Omega_q} |(\nabla + i\tilde{A})\phi|^2 dx - \left(\frac{\hbar^2}{2m_m(\lambda)} \right)' \int_{\Omega_m} |(\nabla + i\tilde{A})\phi|^2 dx \\ &\mp \left(\gamma_q'^B(\lambda) \int_{\Omega_q} |\phi|^2 dx + \gamma_m'^B(\lambda) \int_{\Omega_m} |\phi|^2 dx \right) + \int_{\Omega} |\phi|^2 dx \\ &\geq - \max \left\{ \left(\frac{\hbar^2}{2m_q(\lambda)} \right)', \left(\frac{\hbar^2}{2m_m(\lambda)} \right)' \right\} c(\phi, \phi) - (\max\{|\gamma_q'^B(\lambda)|, |\gamma_m'^B(\lambda)|\} - 1) \int_{\Omega} |\phi|^2 dx \end{aligned}$$

Here we need to consider two cases:

$$\max\{|\gamma_q'^B(\lambda)|, |\gamma_m'^B(\lambda)|\} \leq 1$$

and

$$\max\{|\gamma_q'^B(\lambda)|, |\gamma_m'^B(\lambda)|\} > 1.$$

In the first case the second term becomes negative, which immediately implies that the entire expression is positive completing the argument. Moreover, case 1 also implies the condition (9), as the left hand side of (9) is always positive on J due to the functions $1/m_j(\lambda)$ for $j \in \{q, m\}$ being monotonically falling.

In the second case we continue the above argument as follows

$$\begin{aligned} &\geq \left(-\max \left\{ \left(\frac{\hbar^2}{2m_q(\lambda)} \right)', \left(\frac{\hbar^2}{2m_m(\lambda)} \right)' \right\} - \frac{\max\{|\gamma_q'^B(\lambda)|, |\gamma_m'^B(\lambda)|\} - 1}{\kappa_{min}} \right) c(\phi, \phi) \\ &= \left(-\max \left\{ \left(\frac{\hbar^2}{2m_q(\lambda)} \right)', \left(\frac{\hbar^2}{2m_m(\lambda)} \right)' \right\} - \frac{\max\{|\gamma_q'^B(\lambda)|, |\gamma_m'^B(\lambda)|\} - 1}{\kappa_{min}} \right) \|\phi\|_H^2 > 0. \end{aligned}$$

We remark that for $B = 0$,

$$\max\{|\gamma_q'^B(\lambda)|, |\gamma_m'^B(\lambda)|\} = 0 < 1,$$

implying the existence of the Rayleigh functional. Therefore also this condition is consistent with the previous results. \blacksquare

It follows from [30] that the eigenvalues of (4) in $J = (0, V_m)$ allow a minmax characterization. In general, the eigenvalues of a nonlinear eigenvalue problem have to be specially enumerated for the minmax characterization to hold. However, this ordering coincides with the natural ascending ordering, if the infimum of the Rayleigh functional is contained in J .

Lemma 3.3 *Assume that the conditions of Lemma 3.2 are satisfied. Then it holds that*

$$\inf_{\phi \in D_{\pm}} p_{\pm}(\phi) > 0. \quad (10)$$

Proof: Let $\mu_1^{\pm}(\lambda)$ be the smallest eigenvalue of (5). Then $\mu_1^{\pm}(0) > 0$, and by the continuous dependence of $\mu_1^{\pm}(\lambda)$ on λ there exists $\varepsilon > 0$ such that

$$\frac{a_{\pm}(\phi, \phi; \varepsilon)}{b(\phi, \phi)} \geq \mu_1^{\pm}(\varepsilon) > \frac{1}{2}\mu_1^{\pm}(0) > 0 \quad \text{for every } \phi \in H, \phi \neq 0.$$

Let $\mu_0^{\pm} := \min(\varepsilon, 0.5\mu_1^{\pm}(0))$. Then it follows from the monotonicity of $a_{\pm}(\phi, \phi; \lambda)$ that

$$f(\mu_0^{\pm}; \phi) = \mu_0^{\pm} b(\phi, \phi) - a(\phi, \phi; \mu_0^{\pm}) < 0 \quad \text{for every } \phi \in H, \phi \neq 0,$$

which in turn implies $p_{\pm}(\phi) > \mu_0^{\pm} > 0$ for every $\phi \in D_{\pm}$. Hence (10) holds and therewith

$$\inf_{\phi \in D_{\pm}} p_{\pm}(\phi) \in J. \quad \blacksquare$$

In the next section we proceed to give an equivalent analysis for the rotationally symmetric problem before finally stating the minmax principle for both problems in Section 5.

4 Axially symmetric Hamiltonian

In this section we derive the stationary Schrödinger equation governing the electronic levels of the axially symmetric quantum structures. Due to the symmetry we can separate off the angular direction and consider a sequence of two dimensional problems in the (r, z) plane instead. For the plane problem let $\Omega, \Omega_q, \Omega_m$ and the boundaries $\partial\Omega, \partial\Omega_q, \partial\Omega_m$ denote their restrictions to the (r, z) plane. We consider an elliptical quantum ring, Ω_q , obtained by a revolution around the z -axis of an ellipse centered at (r_0, z_0) with principal axes a (along the r -axis) and b (along z -axis), centrally embedded in a cylindrical matrix, Ω_m , of radius R_m and height Z_m . The quantum ring and the matrix are displayed in Figure 2.

To separate the angular direction we rewrite the stationary Schrödinger equation (2) in cylindrical coordinates choosing the gauge $A = \frac{1}{2}(B \times \mathbf{r})$, where \mathbf{r} denotes the point vector (θ, r, z)

$$-\frac{\hbar^2}{2m_j(\lambda)} \left[\frac{1}{r} \frac{\partial}{\partial r} \left(r \frac{\partial \Phi}{\partial r} \right) + \frac{1}{r^2} \frac{\partial^2 \Phi}{\partial \theta^2} + \frac{\partial^2 \Phi}{\partial z^2} \right] + \frac{e^2}{8m_j(\lambda)} (B \times \mathbf{r})^2 \quad (11)$$

$$-\frac{i\hbar e}{2m_j(\lambda)} (B \times \mathbf{r}) \cdot \nabla \Phi + \sigma_z \frac{\mu_B}{2} B g_j(\lambda) \Phi + V_j \Phi = \lambda \Phi, \quad j \in \{q, m\}.$$

Due to the radial symmetry of the problem we expect a solution of the following type

$$\Phi(\theta, r, z) = \phi(r, z)\psi(\theta). \quad (12)$$

Substituting (12) in (11) and separating the variables we obtain two independent equations [25]

$$\frac{\hbar^2}{2m_j(\lambda)} \left[\frac{\partial}{\partial r} \left(-r \frac{\partial \phi(r, z)}{\partial r} \right) - r \frac{\partial^2 \phi(r, z)}{\partial z^2} + \frac{\ell^2}{r} \phi(r, z) \right] + \frac{e^2 B^2}{8m_j(\lambda)} r^3 \phi(r, z) \quad (13)$$

$$+ \ell B \frac{\hbar e}{2m_j(\lambda)} r \phi(r, z) + \sigma_z \frac{\mu_B}{2} B g_j(\lambda) r \phi(r, z) + (V_j - \lambda) r \phi(r, z) = 0,$$

$$\frac{\partial^2 \psi(\theta)}{\partial \theta^2} + \ell^2 \psi(\theta) = 0 \quad (14)$$

Here we made use of the definition of the angular momentum

$$L = \mathbf{r} \times (-i\hbar \nabla)$$

along with the fact that its projection on the z -axis is quantized by the angular quantum number ℓ , i.e. $L \cdot B = \ell \hbar B$.

The solution of the second equation (14) is well known to be a plane wave

$$\psi_\ell(\theta) = \exp(i\ell\theta), \quad \ell = 0, \pm 1, \pm 2, \dots,$$

while the first equation (13) is a nonlinear eigenvalue problem in the plane defined by r and z .

On the outer boundary of the matrix, $\partial\Omega$, the homogeneous Dirichlet conditions, and on the dot matrix interface, Ω_{int} , the BenDaniel-Duke conditions are inherited from the three dimensional problem. On the rotational axis, $\partial\Omega_{rot}$, for continuity reasons we assume the homogeneous Neumann conditions $\frac{\partial\phi}{\partial r} = 0$ for $\ell = 0$ and the homogeneous Dirichlet conditions $\phi = 0$ for $\ell \neq 0$.

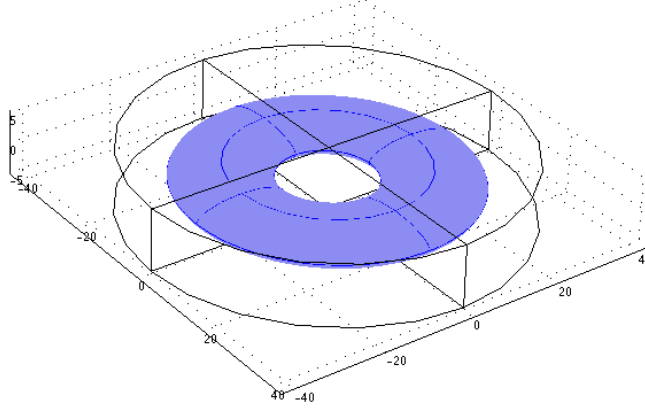


Figure 2: Elliptical quantum ring embedded in a cylindrical matrix.

The eigenvalues of each of the three dimensional problems (11) with $\sigma_z = \pm 1$, respectively, are the ordered eigenvalues of the sequence of the matching two dimensional problems (13) corresponding to the quantum numbers $\ell = 0, \pm 1, \pm 2, \dots$. The eigenfunctions of (11) have the following form

$$\Phi(\theta, r, z) = \phi_{\ell, \sigma_z}(r, z) \exp(i\ell\theta),$$

where $\phi_{\ell, \sigma_z}(r, z)$ is an eigenfunction of the corresponding plane problem. Henceforth for the simplicity of notation we omit the indexing of the eigenfunctions indicating the dependence on ℓ and σ_z .

In the presence of the magnetic field the electronic levels split, which leads to a pair for $\ell = 0$ and a quadruple for $\ell \neq 0$ of plane problems to be solved which differ by the sign of the third and fourth term in (13). Problems of this type were also numerically investigated by other authors by means of Full Approximation Methods (FAM) [12, 13, 14, 24], which are substantially less efficient than the iterative projection methods presented here. For comparison of FAM type methods with iterative projection methods see Section 4.3 in [4]. In contrast without the magnetic field, $B = 0$, there is only one problem to solve for each $|\ell|$. The iterative projection methods for rotationally symmetric quantum dots in the absence of magnetic field are discussed in Chapter 4 of [4].

We now proceed to give an analysis for the axially symmetric problem analogous to that of the general three dimensional case in Section 3.

$$\text{Let } \Omega := (0, R_m) \times (-Z_m/2, Z_m/2), \Omega_q := \left\{ (r, z) : \frac{(r-r_0)^2}{a^2} + \frac{(z-z_0)^2}{b^2} < 1 \right\},$$

and $\Omega_m := \Omega \setminus \bar{\Omega}_q$. Due to the term $\frac{\ell^2}{r}$ it is necessary to distinguish two cases $\ell = 0$ and $\ell \neq 0$, since the trial function spaces in the variational formulation are different.

For $\ell = 0$, since the splitting of the energy levels is only due to the Zeeman term, it is appropriate to describe the problem in the weighted Sobolev space

$$H^0 := \left\{ \phi \in L^2(\Omega) : r|\nabla\phi|^2 \in L^1(\Omega), \quad \begin{array}{l} \phi(r, \pm Z_m/2) = 0, \quad 0 \leq r \leq R_m, \\ \phi(R_m, z) = 0, \quad -Z_m/2 \leq z \leq Z_m/2 \end{array} \right\}$$

with the scalar product

$$\langle \phi, \psi \rangle_{H^0} := \int_{\Omega} r \nabla \phi \cdot \nabla \psi \, d(r, z),$$

and the weighted Lebesgue space

$$W := \{ \phi : r|\phi|^2 \in L^1(\Omega) \} \quad \text{with} \quad \langle \phi, \psi \rangle_W := \int_{\Omega} r \phi \psi \, d(r, z).$$

Then H^0 is compactly embedded in W (cf. [21], Theorem. 7.13(ii), Remark 7.14(i)).

For $\ell \neq 0$ the following environment is appropriate. Let H^ℓ be the weighted Sobolev space

$$H^\ell = H_0^1(\Omega; r^{-1}, r) := \{ \phi : \frac{1}{r}|\phi|^2 \in L^1(\Omega), \quad r|\nabla\phi|^2 \in L^1(\Omega), \quad \phi = 0 \text{ on } \partial\Omega \}$$

with the standard inner product

$$\langle \phi, \psi \rangle_{H^\ell} := \int_{\Omega} r \nabla \phi \cdot \nabla \psi + \frac{1}{r} \phi \psi \, d(r, z)$$

and we define W as in case $\ell = 0$. Then by [21], Theorem. 18.12 and Example. 18.15, H^ℓ is compactly embedded in W . For the details of both embedding arguments see Section 4.2 of [4].

For the simplicity of the notation, from now on we refer to the appropriate trial function space using the conditional space definition

$$H := \begin{cases} H^0, & \ell = 0, \\ H^\ell, & \ell \neq 0. \end{cases}$$

Multiplying equation (13) by $\psi \in H$ and integrating by parts, we obtain the variational form of the Schrödinger equation (13)

Find $\lambda \in J$ and $\phi \in H$, $\phi \neq 0$ such that

$$\begin{aligned}
 a_{\pm}^{\ell}(\phi, \psi; \lambda) &:= \frac{\hbar^2}{2m_q(\lambda)} \int_{\Omega_q} \left(r \nabla \phi \cdot \nabla \psi + \frac{\ell^2}{r} \phi \psi + \frac{\mathcal{B}^2}{4} r^3 \phi \psi \right) d(r, z) \\
 &+ \frac{\hbar^2}{2m_m(\lambda)} \int_{\Omega_m} \left(r \nabla \phi \cdot \nabla \psi + \frac{\ell^2}{r} \phi \psi + \frac{\mathcal{B}^2}{4} r^3 \phi \psi \right) d(r, z) \\
 &\pm \left(\gamma_q^B(\lambda) \int_{\Omega_q} r \phi \psi d(r, z) + \gamma_m^B(\lambda) \int_{\Omega_m} r \phi \psi d(r, z) \right) \\
 &\pm |\ell \mathcal{B}| \left(\frac{\hbar^2}{2m_q(\lambda)} \int_{\Omega_q} r \phi \psi d(r, z) + \frac{\hbar^2}{2m_m(\lambda)} \int_{\Omega_m} r \phi \psi d(r, z) \right) \\
 &+ V_m \int_{\Omega_m} r \phi \psi d(r, z) \\
 &= \lambda \int_{\Omega} r \phi \psi d(r, z) =: \lambda b(\phi, \psi) \quad \text{for every } \psi \in H, \tag{15}
 \end{aligned}$$

where $\mathcal{B} = \frac{eB}{\hbar}$ and $\gamma_j^B(\lambda)$ was defined in Section 3.

The bilinear form $b(\cdot, \cdot)$ is obviously positive and bounded on W . We recall from Section 3 that $E_{g,j} - V_j > 0$ and therefore the functions $\lambda \mapsto \frac{1}{m_j(\lambda)}$ are defined for $\lambda \geq 0$ (hence in J), and are positive and monotonically decreasing and for $B > 0$ $\gamma_j^B(\lambda)$ are monotonically increasing and bounded on J . The bilinear form $a_{\pm}^{\ell}(\cdot, \cdot; \lambda)$ is symmetric and the boundedness immediately follows from the compact embedding of H into W and the boundedness of $\lambda \mapsto \frac{1}{m_j(\lambda)}$ and $\gamma_j^B(\lambda)$ on J .

Lemma 4.1 gives a sufficient condition for $a_{\pm}^{\ell}(\cdot, \cdot; \lambda)$, to be H -elliptic, thus for fixed $\lambda \in J$ the linear eigenvalue problem

$$\text{Find } \mu^{\ell} \text{ and } \phi \in H, \phi \neq 0 \text{ with } a_{\pm}^{\ell}(\phi, \psi; \lambda) = \mu^{\ell} b(\phi, \psi) \quad \text{for every } \psi \in H$$

has a countable set of eigenvalues $0 < \mu_1^{\ell \pm} \leq \mu_2^{\ell \pm} \leq \dots$ which can be characterized as minmax values of the Rayleigh quotient (cf. [2]):

$$\mu_j^{\ell \pm} = \min_{V \subset H, \dim V = j} \max_{\phi \in V, \phi \neq 0} \frac{a_{\pm}^{\ell}(\phi, \phi; \lambda)}{b(\phi, \phi)}.$$

Lemma 4.1 *Let κ_{\min} be the smallest eigenvalue of the following eigenvalue problem*

$$c^{\ell}(\phi, \psi) := \int_{\Omega} \left(r \nabla \phi \cdot \nabla \psi + \frac{\ell^2}{r} \phi \psi + \frac{\mathcal{B}^2}{4} r^3 \phi \psi \right) d(r, z) = \kappa \int_{\Omega} r \phi \psi d(r, z) \tag{16}$$

for every $\psi \in H$. If

$$\min \left\{ \frac{\hbar^2}{2m_q(\lambda)}, \frac{\hbar^2}{2m_m(\lambda)} \right\} > \frac{\max\{\omega_q^B(\lambda), \omega_m^B(\lambda)\}}{\kappa_{\min}} \quad \text{for every } \lambda \in J, \quad (17)$$

where $\omega_j^B(\lambda) = |\gamma_j^B(\lambda)| - V_j + |\ell\mathcal{B}|\frac{\hbar^2}{2m_j(\lambda)}$, then $a_{\pm}^{\ell}(\cdot, \cdot; \lambda)$ is H -elliptic for every fixed $\lambda \in J$.

Proof: Similarly as in the proof of Lemma 3.1 for $\phi \in H$ it holds

$$\begin{aligned} a_{\pm}^{\ell}(\phi, \phi; \lambda) &\geq \min \left\{ \frac{\hbar^2}{2m_q(\lambda)}, \frac{\hbar^2}{2m_m(\lambda)} \right\} c^{\ell}(\phi, \phi) - \left(|\gamma_q^B(\lambda)| + \frac{|\ell\mathcal{B}|\hbar^2}{2m_q(\lambda)} \right) \int_{\Omega_q} r\phi^2 d(r, z) \\ &\quad - \left(|\gamma_m^B(\lambda)| - V_m + \frac{|\ell\mathcal{B}|\hbar^2}{2m_m(\lambda)} \right) \int_{\Omega_m} r\phi^2 d(r, z) \\ &\geq \min \left\{ \frac{\hbar^2}{2m_q(\lambda)}, \frac{\hbar^2}{2m_m(\lambda)} \right\} c^{\ell}(\phi, \phi) - \max\{\omega_q^B(\lambda), \omega_m^B(\lambda)\} \int_{\Omega} r\phi^2 d(r, z) \\ &\geq \left(\min \left\{ \frac{\hbar^2}{2m_q(\lambda)}, \frac{\hbar^2}{2m_m(\lambda)} \right\} - \frac{\max\{\omega_q^B(\lambda), \omega_m^B(\lambda)\}}{\kappa_{\min}} \right) c^{\ell}(\phi, \phi) \\ &\geq \left(\min \left\{ \frac{\hbar^2}{2m_q(\lambda)}, \frac{\hbar^2}{2m_m(\lambda)} \right\} - \frac{\max\{\omega_q^B(\lambda), \omega_m^B(\lambda)\}}{\kappa_{\min}} \right) \|\phi\|_H^2. \end{aligned}$$

We observe that if $B = 0$ then the right hand side of the condition (17) becomes 0, thus (17) is trivially satisfied since $\lambda \rightarrow \frac{1}{m_j(\lambda)}$ for $j \in \{q, m\}$ are positive on J . This is again consistent with our earlier variational results for rotationally symmetric structures in the absence of the magnetic field in Chapter 4 of [4]. \blacksquare

As in Section 3 we require the existence of a Rayleigh functional p_{\pm}^{ℓ} , which is a solution of the corresponding equation

$$f_{\pm}^{\ell}(\lambda; \phi) := \lambda b(\phi, \phi) - a_{\pm}^{\ell}(\phi, \phi; \lambda) = 0.$$

The sufficient condition for its existence is given by the following lemma.

Lemma 4.2 *Assume that the conditions of Lemma 4.1 hold, and*

$$-\frac{\hbar^2}{2} \max \left\{ \left(\frac{1}{m_q(\lambda)} \right)', \left(\frac{1}{m_m(\lambda)} \right)' \right\} > \frac{\max\{\eta_q^B(\lambda), \eta_m^B(\lambda)\} - 1}{\kappa_{\min}} \quad \text{for every } \lambda \in J, \quad (18)$$

where $\eta_j^B(\lambda) = |\gamma_j^B(\lambda)| - |\ell\mathcal{B}|\left(\frac{\hbar^2}{2m_j(\lambda)}\right)'$ and κ_{\min} denotes the smallest eigenvalue of the eigenvalue problem (16).

Then for every $\phi \in H$, $\phi \neq 0$ each of the real equations

$$f_{\pm}^{\ell}(\lambda; \phi) := \lambda b(\phi, \phi) - a_{\pm}^{\ell}(\phi, \phi; \lambda) = 0$$

has at most one solution $p_{\pm}^{\ell}(\phi) \in J$ and $\inf_{\phi \in D_{\pm}^{\ell}} p_{\pm}^{\ell}(\phi) \in J$ for the domain of definition $D_{\pm}^{\ell} \subset H \setminus \{0\}$ of p_{\pm}^{ℓ} .

Proof: Similarly to the proof of Lemma 3.2 we show that $f_{\pm}^{\ell}(0; \phi) < 0$ and $\frac{\partial}{\partial \lambda} f_{\pm}^{\ell}(\lambda, \phi) > 0$ for every $\phi \in H$, $\phi \neq 0$ and every $\lambda \in J$.

Since, $f_{\pm}^{\ell}(0; \phi) = -a_{\pm}^{\ell}(\phi, \phi; 0)$ and $a_{\pm}^{\ell}(\phi, \phi; 0)$ is elliptic it immediately follows $f_{\pm}^{\ell}(0; \phi) < 0$. Let $D_{\pm}^{\ell} = \{\phi \in H \setminus \{0\} : p_{\pm}^{\ell}(\phi) \in J\}$ then arguing as in the proof of Lemma 3.3 we obtain $\inf_{\phi \in D_{\pm}^{\ell}} p_{\pm}^{\ell}(\phi) \in J$.

For every $\phi \in H$, $\phi \neq 0$ and every $\lambda \in J$ similarly as in the proof of Lemma 3.2 it follows

$$\begin{aligned} \frac{\partial}{\partial \lambda} f_{\pm}^{\ell}(\lambda; \phi) &\geq \int_{\Omega} r \phi^2 d(r, z) - \left(\frac{\hbar^2}{2m_q(\lambda)} \right)' \int_{\Omega_q} \left(r |\nabla \phi|^2 + \frac{\ell^2}{r} \phi^2 + \frac{\mathcal{B}^2}{4} r^3 \phi^2 \right) d(r, z) \\ &- \left(\frac{\hbar^2}{2m_m(\lambda)} \right)' \int_{\Omega_m} \left(r |\nabla \phi|^2 + \frac{\ell^2}{r} \phi^2 + \frac{\mathcal{B}^2}{4} r^3 \phi^2 \right) d(r, z) \\ &- \left(|\gamma_q^{\prime B}(\lambda)| - \left(\frac{|\ell \mathcal{B}| \hbar^2}{2m_q(\lambda)} \right)' \right) \int_{\Omega_q} r \phi^2 d(r, z) - \left(|\gamma_m^{\prime B}(\lambda)| - \left(\frac{|\ell \mathcal{B}| \hbar^2}{2m_m(\lambda)} \right)' \right) \int_{\Omega_m} r \phi^2 d(r, z) \\ &\geq -\frac{\hbar^2}{2} \max \left\{ \left(\frac{1}{m_q(\lambda)} \right)', \left(\frac{1}{m_m(\lambda)} \right)' \right\} c^{\ell}(\phi, \phi) - (\max \{ \eta_q^B(\lambda), \eta_m^B(\lambda) \} - 1) \int_{\Omega} r \phi^2 d(r, z) \end{aligned}$$

Similarly, as in the proof of Lemma 3.2 we distinguish two cases

$$\max \{ \eta_q^B(\lambda), \eta_m^B(\lambda) \} \leq 1$$

and

$$\max \{ \eta_q^B(\lambda), \eta_m^B(\lambda) \} > 1.$$

As in Lemma 3.2 in the first case the positivity follows immediately, at the same time implying the condition (18).

In the second case, we continue the above argument as follows

$$\geq \left(-\frac{\hbar^2}{2} \max \left\{ \left(\frac{1}{m_q(\lambda)} \right)', \left(\frac{1}{m_m(\lambda)} \right)' \right\} - \frac{\max \{ \eta_q^B(\lambda), \eta_m^B(\lambda) \} - 1}{\kappa_{min}} \right) c^{\ell}(\phi, \phi) > 0.$$

For $B = 0$, we have

$$\max \{ \eta_q^B(\lambda), \eta_m^B(\lambda) \} = 0 < 1,$$

and the case 1 implies the existence of the Rayleigh functional. Again this is consistent with the results for the magnetic field free case as described in Chapter 4 of [4]. \blacksquare

5 Minmax principle

Finally, we are in the position to formulate the minmax principle for both nonlinear eigenvalue problems (4) and (15). For the compactness of notation we henceforth drop the superscript ℓ for the plane problem.

Under the conditions of Lemma 3.2 or Lemma 4.2 for each of the eigenvalue problems in (4) and (15), the Rayleigh functional

$$p_{\pm} : H \supset D_{\pm} \rightarrow J$$

is defined. The general conditions of the minmax theory for nonlinear eigenvalue problems in [30] are satisfied, and Theorems 2.1 and 2.9 of [30] imply the following characterization of the eigenvalues of (4) and (15) in the interval J .

Theorem 5.1 *Assume that the conditions of Lemma 3.2 or Lemma 4.2, respectively, are satisfied. Then each of the Schrödinger equations in (4) and (15), has a finite number of eigenvalues in J , and it holds that*

(i) *The k th smallest eigenvalue can be characterized by*

$$\lambda_k^{\pm} = \min_{\dim V=k, V \cap D_{\pm} \neq \emptyset} \max_{\phi \in V \cap D_{\pm}} p_{\pm}(\phi). \quad (19)$$

(ii) *The minimum in (19) is attained for the subspace which is spanned by eigenfunctions corresponding to the k smallest eigenvalues of the linear eigenproblem*

$$a_{\pm}(\phi, \psi; \lambda_k^{\pm}) = \mu b(\phi, \psi) \quad \text{for every } \psi \in H. \quad (20)$$

Equipped with this result we can devise efficient iterative projection methods which compute approximations to the eigenvalues of the nonlinear problem safely one after another and without repeated convergence to already computed eigenpairs, as it can be achieved in the linear case. To apply numerical methods we discretize the Schrödinger equations by a Rayleigh-Ritz method (e.g. finite elements), thus for the three dimensional problem we obtain a rational matrix eigenvalue problem of the following type

$$\begin{aligned} S_{\pm}(\lambda)x &:= \lambda Mx - \frac{\hbar^2}{2m_q(\lambda)} K_q x - \frac{\hbar^2}{2m_m(\lambda)} K_m x - V_m M_m x \\ &\pm (\gamma_q^B(\lambda) M_q + \gamma_m^B(\lambda) M_m)x = 0, \end{aligned} \quad (21)$$

and the involved matrices are given by the integrals of the products of the shape functions $\phi_i, i \in 1, \dots, n$ and their derivatives

$$\begin{aligned} K_j^{(i,k)} &= \int_{\Omega_j} (\nabla + i\tilde{A})\phi_i \overline{(\nabla + i\tilde{A})\phi_k} dx, \quad j \in \{q, m\} \\ M^{(i,k)} &= \int_{\Omega} \phi_i \bar{\phi}_k dx \quad \text{and} \quad M_j^{(i,k)} = \int_{\Omega_j} \phi_i \bar{\phi}_k dx. \end{aligned}$$

In the axially symmetric case we arrive at the following rational matrix eigenvalue problem

$$S_{\pm}^{\ell}(\lambda)x := \lambda Mx - \frac{\hbar^2}{2m_q(\lambda)}K_q x - \frac{\hbar^2}{2m_m(\lambda)}K_m x - V_m M_m x \\ \pm (\gamma_q^B(\lambda)M_q + \gamma_m^B(\lambda)M_m)x \pm |\ell\mathcal{B}| \left(\frac{\hbar^2}{2m_q(\lambda)}M_q + \frac{\hbar^2}{2m_m(\lambda)}M_m \right) x = (\mathfrak{B})$$

where

$$K_j^{(i,k)} = \int_{\Omega_j} \left(r \nabla \phi_i \nabla \phi_k + \frac{\ell^2}{r} \phi_i \phi_k + \frac{\mathcal{B}^2}{4} r^3 \phi_i \phi_k \right) d(r, z), \quad j \in \{q, m\} \\ M^{(i,k)} = \int_{\Omega} r \phi_i \phi_k d(r, z) \quad \text{and} \quad M_j^{(i,k)} = \int_{\Omega_j} r \phi_i \phi_k d(r, z).$$

The following corollary is an obvious consequence of the Theorem 5.1, where we again skipped the superscript ℓ for the compactness of notation.

Corollary 5.1 *For each of the discretized problems in (21) and (22) the discrete versions of the conditions of Lemma 3.2 and 4.2, respectively, are sufficient for the existence of Rayleigh functionals q_{\pm} corresponding to S_{\pm} on the interval J , and the eigenvalues of S_{\pm} in J are minmax values of q_{\pm} . Moreover, it follows from the minmax characterization that the k th smallest eigenvalue of S_{\pm} is an upper bound for the corresponding eigenvalue of the original continuous problem in (4) and (15), respectively.*

6 Solving the nonlinear eigenvalue problem

In this section we consider the problem to compute few eigenvalues and the corresponding eigenvectors at the lower end of the spectrum of the discretization (21) or (22) of the Schrödinger equation. Since the described numerical methods apply to all of the discrete problems S_{\pm} , S_{\pm}^{ℓ} in the remainder of this section we omit any sub- and superscripts and refer to the discretized eigenvalue problem to be solved by $S(\lambda)x = 0$.

For large scale linear sparse eigenproblems the methods of choice are iterative projection methods like for instance Lanczos, Arnoldi, or Jacobi-Davidson. In such methods the approximations to the wanted eigenvalues and eigenvectors are extracted from projections of the eigenproblem to a series of nested, low dimensional subspaces built in the course of the algorithm.

Let $V \in \mathbb{R}^{n \times k}$ be an (orthonormal) basis of the current search space $\mathcal{V} \subset \mathbb{R}^n$, and assume that (θ, y) , $y \in \mathbb{R}^k$ is an eigenpair of the projected eigenvalue problem

$$V^T S(\lambda) V y = 0,$$

and denote by $x := Vy$ the corresponding Ritz vector. To obtain an improved approximation it is reasonable to expand \mathcal{V} in a direction with a high approximation potential for the eigenvector wanted next.

In the literature one comes across in general two strategies for the subspace expansion: the Jacobi-Davidson type methods like [23] for the polynomial and [7] for the general nonlinear eigenvalue problem and the methods based on the residual inverse iteration, like the Nonlinear Arnoldi method [28] for general nonlinear eigenvalue problem or the Quadratic Arnoldi method [18, 19] for the special case of the quadratic eigenvalue problem. In this work we restrict ourselves to the latter type of methods, in particular to the Nonlinear Arnoldi method as the problems at hand are rational eigenvalue problems. This decision is based on our numerical experience (see Section 3.5 in [4] for detailed discussion) that for problems with relatively small number of confined states and of moderate size i.e. which size still allows for computation of a good quality preconditioner the Nonlinear Arnoldi method performs superior to the Jacobi Davidson type methods.

Residual inverse iteration, introduced by Neumaier [20], suggests the expansion

$$v = S(\sigma)^{-1}S(\theta)x,$$

of the search space \mathcal{V} , where σ is a fixed parameter close to the wanted eigenvalues.

For a linear eigenproblem $S(\lambda) = A - \lambda B$ this is exactly the Cayley transformation with the pole σ and the zero θ , and since $(A - \sigma B)^{-1}(A - \theta B) = I + (\sigma - \theta)(A - \sigma B)^{-1}B$ and due to shift-invariance of Krylov spaces the resulting projection method expanding \mathcal{V} by v is nothing else but the shift-and-invert Arnoldi method.

If the linear system $S(\sigma)v = S(\theta)x$ is too expensive to solve for v we may choose as new direction $v = K^{-1}S(\theta)x$ with $K \approx S(\sigma)$, and for the linear problem we obtain an inexact Cayley transformation or a preconditioned Arnoldi method. The resulting iterative projection method given in Algorithm 1, is therefore called nonlinear Arnoldi method, although no Krylov space is constructed and no Arnoldi recursion holds.

There are many details that have to be considered when implementing the nonlinear Arnoldi method concerning the choice of the initial basis, when and how to update the preconditioner, and how to restart the method. A detailed discussion is given in [28].

Applying iterative projection method to a general nonlinear eigenvalue problem while approximating more than one eigenpair, it is crucial to prevent the algorithm from converging to the same eigenpair repeatedly, which in turn may negatively affect the convergence speed. For linear eigenvalue problems this is easily achieved by using Schur forms or generalized Schur forms for the projected problem and then locking or purging certain eigenvectors. For nonlinear problems, though, such normal forms do not exist thus presenting a challenge in maintaining good convergence properties.

However, as it can be seen from Theorem 5.1 the eigenvalues of a symmetric

Algorithm 1 Nonlinear Arnoldi Method

- 1: start with an initial pole σ and an initial orthonormal basis V , $V^T V = I$
 - 2: determine preconditioner $K \approx S(\sigma)$, σ close to the smallest eigenvalue
 - 3: $k=1$
 - 4: **while** $k \leq$ number of wanted eigenvalues **do**
 - 5: compute the k th smallest eigenvalue μ and the corresponding normalized eigenvector y of the projected problem $V^T S(\mu) V y = 0$
 - 6: compute the Ritz vector $u = V y$ and the residual $r = S(\mu) u$
 - 7: **if** $\|r\| < \varepsilon$ **then**
 - 8: accept eigenvalue $\lambda_k = \mu$, and eigenvector $x_k = u$,
 - 9: choose new pole σ and update preconditioner $K \approx S(\sigma)$ if indicated
 - 10: restart if necessary
 - 11: $k = k + 1$
 - 12: **end if**
 - 13: solve $K v = r$ for v
 - 14: $v = v - V V^T v$, $\tilde{v} = v / \|v\|$, $V = [V, \tilde{v}]$
 - 15: reorthogonalize if necessary
 - 16: **end while**
-

nonlinear eigenproblem satisfying a minmax characterization can be computed safely one after another. Theorem 5.1 builds up the connection between the nonlinear eigenvalue problem and the linear eigenvalue problem (20) resulting from fixing the eigenvalue parameter λ on the left hand side of (4),(15), thereby paving the way to exploiting the good numerical properties of the linear symmetric eigenvalue problem to target the nonlinear eigenvalue with a specific number. For instance, for the k th eigenpair the minimum in (19) is attained for the invariant subspace of $S(\lambda_k)$ corresponding to its k largest eigenvalues, and the maximum by every linear eigenvector of $S_k(\lambda_k)$ corresponding to the eigenvalue 0. Exactly this property is at the core of the safeguarded iteration for computing the k th smallest eigenvalue of the projected nonlinear problem $P(\lambda)y := V^T S(\lambda) V y = 0$. The pseudocode for the safeguarded iteration is given in Algorithm 2.

Algorithm 2 Safeguarded iteration

- 1: start with an approximation μ_1 to the k th smallest eigenvalue of $P(\lambda)y = 0$
 - 2: **for** $j = 1, 2, \dots$ until convergence **do**
 - 3: determine an eigenvector y corresponding to the k th largest eigenvalue of the matrix $P(\mu_j)$
 - 4: evaluate $\mu_{j+1} = q(y)$, i.e. solve $y^T P(\mu_{j+1}) y = 0$ for μ_{j+1}
 - 5: **end for**
-

The safeguarded iteration has very good convergence properties [27]: It converges globally to the smallest eigenvalue λ_1 . The (local) convergence to simple eigenvalues is quadratic. If $P'(\lambda)$ is positive definite, and y in Step 3 of Al-

gorithm 2 is replaced by an eigenvector of $P(\mu_j)y = \mu P'(\mu_j)y$ corresponding to the k th largest eigenvalue, then the convergence is even cubic. Moreover, a variant exists which is globally convergent also for higher eigenvalues, Chapter 7 in [4], [16].

7 Efficient solution of the pair/quadruple of non-linear eigenvalue problems

So far, we derived conditions which guarantee that one particular problem of the type (4) or (15) allows for a minmax characterization of its eigenvalues. If they hold for the problem in question we can apply an iterative projection method like Nonlinear Arnoldi or Jacobi Davidson and solve each of the problems for $\sigma_z \in \{-1, 1\}$ and in the axial symmetric case also for ℓ and $-\ell$ separately. However, as we show in this section we can do significantly better treating a pair/quadruple of the problems simultaneously, as from our physical intuition we expect the eigensolutions for $\sigma_z = 1$ and $\sigma_z = -1$ and for ℓ and $-\ell$ to be highly related.

In the following we consider two examples: a pyramidal quantum dot and an axially symmetric quantum ring. The matrices for the discretized problem S_{\pm} were obtained with COMSOL [10] and all the computations were run under MATLAB 7.3 on an Intel Pentium D processor with 4 GByte RAM and 3.2 GHz.

7.1 Pyramidal quantum dot

Our first example is a pyramidal quantum dot (cf. Figure 1) of height 6.2nm and width 12.4nm embedded into a cuboid matrix $24.8 \times 24.8 \times 18.6 \text{ nm}^3$, which we expose to a homogenous magnetic field of strengths 1, 5, 10, 15, 20, 25[T] directed along the z -axis.

The pyramid and the matrix are discretized on a tetrahedral grid with quadratic Lagrangian elements. The eigenfunctions decay rapidly outside of the dot and the coefficient functions of the differential operator have a jump on the interface. We therefore chose a nonuniform grid, which is fine on the interface between the dot and the matrix, while coarser on the interior of dot and the matrix. In this way we obtained a pair of rational matrix eigenvalue problems (21) with 46291 degrees of freedom.

Before we apply an iterative projection method, we need to check the conditions (7) and (9) which guarantee the minmax characterization of the eigenvalues of (4). In fact, since we are to apply the method to the discrete problem their discrete counterparts are enough to ensure the convergence of the iterative projection method. The discrete eigenvalue problem corresponding to (6) reads

$$Kx = \kappa Mx, \quad (23)$$

where K depends on B . The smallest eigenvalue of (23) for different values of

B is displayed in Table 2. The condition (7) holds if

$$\kappa_{min} > \frac{\max \{ |\gamma_q^B(\lambda)|, |\gamma_m^B(\lambda)| - V_m \}}{\min \left\{ \frac{\hbar^2}{2m_q(\lambda)}, \frac{\hbar^2}{2m_m(\lambda)} \right\}} \quad \text{for every } \lambda \in J. \quad (24)$$

At this stage we can utilize the properties of the involved functions. The functions $\gamma_j^B(\lambda)$ are monotonic but $|\gamma_j^B(\lambda)|$ are not in general. In fact $|\gamma_q^B(\lambda)|$ is monotonically falling function while $|\gamma_m^B(\lambda)|$ hits the real axis, see Figure 3. However,

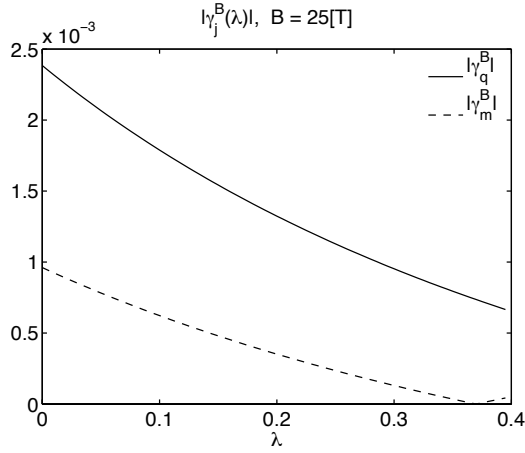


Figure 3: $|\gamma_j^B(\lambda)|, j \in \{q, m\}$ for $B = 25[\text{T}]$ on the interval $J = (0, 0.395)$. Note, that B enters only as a multiplicative factor, thus it does not change the properties of the function.

$$\max \{ |\gamma_q^B(\lambda)|, |\gamma_m^B(\lambda)| - V_m \} = |\gamma_q^B(\lambda)|$$

thus together with $\frac{\hbar^2}{2m_j(\lambda)}$ and $|\gamma_q^B(\lambda)|$ being monotonically falling, the right hand side can be bounded on J as

$$\kappa_{min} > \frac{|\gamma_q^B(0)|}{\min \left\{ \frac{\hbar^2}{2m_q(V_m)}, \frac{\hbar^2}{2m_m(V_m)} \right\}}, \quad (25)$$

which is a sufficient condition for (24). Since the right hand side of (25) is in fact a multiple of B

$$\frac{|\gamma_q^B(0)|}{\min \left\{ \frac{\hbar^2}{2m_q(V_m)}, \frac{\hbar^2}{2m_m(V_m)} \right\}} \approx 0.167 \cdot 10^{-3} B$$

we obtain a bound on κ_{min} in dependence of B

$$\kappa_{min} > 0.167 \cdot 10^{-3} B.$$

Table 2: The smallest eigenvalue of (23) for different strengths of magnetic field B .

B [T]	1	5	10	15	20	25
κ_{min}	0.0607	0.0612	0.0629	0.0656	0.0693	0.0739

 Table 3: Singular values of $[X_-, X_+]$.

B [T]	σ_1	σ_2	σ_3	σ_4	σ_5
5	1.5085	1.4151	1.4133	1.3132	0.0003
15	1.5096	1.4151	1.4132	1.3119	0.0007
25	1.4194	1.4146	1.4133	1.4095	0.0012

This is satisfied for all magnetic field strengths in the range $0 - 25$ [T]. Further, from Table 2, we estimate $\kappa_{min} < 0.1$ for all realistic strengths of magnetic field. With such κ_{min} it follows that the maximal magnetic field strength, for which the condition (25) remains intact is larger than 500 [T].

The second condition (9) secures the existence of the Rayleigh functional. First we check, whether

$$\max \left\{ \left| \gamma_q^{B'}(\lambda) \right|, \left| \gamma_m^{B'}(\lambda) \right| \right\} \leq 1.$$

Since $\gamma_j^{B'}(\lambda)$ are positive monotonically falling functions

$$\max_{\lambda \in J} \left\{ \left| \gamma_q^{B'}(\lambda) \right|, \left| \gamma_m^{B'}(\lambda) \right| \right\} = \max \left\{ \gamma_q^{B'}(0), \gamma_m^{B'}(0) \right\} \approx 0.27 \cdot 10^{-3} B,$$

which remains smaller than 1 for all $B < 3700$ [T] and implies the monotonicity condition.

The physical background of the problem, i.e. the splitting of the electronic levels suggests that the eigenfunctions of the pair of problems have some common directions. This conjecture is also supported by the structure of the Zeeman term in (4) which involves the sesquilinear form $b_j(\cdot, \cdot)$ and therefore bears some similarity to a “shift”.

To verify our guess we perform the following experiment. We assemble four eigenvectors X_- and X_+ corresponding to the problem S_- and S_+ , respectively, in one matrix and compute its singular value decomposition. The singular values are shown in Table 3 for different values of the magnetic field strength B .

For all three values of B we observe a clear gap between the 4th and the 5th singular value whereas neither the singular values of X_+ nor those of X_- contain an essential gap. This indicates that the eigensubspaces X_- and X_+ overlap substantially. Though this effect wears off with growing B it is still of the order 10^{-3} for a very large $B = 25$ [T].

In view of this experiment it appears that solving the pair of problems S_{\pm} simultaneously allows the solution of one problem to benefit from the solution of the other. This leads to the following approach. We apply an iterative projection method to both problems simultaneously in such a way that they use the same search space \mathcal{V} . There are many ways of combining these iterations. We just name the following three:

1. **Fast alternating:** We expand the search space using the residual corresponding to the S_+ and S_- , alternatingly, while iterating the corresponding eigenpairs of S_+ and S_- simultaneously;
2. **Slow alternating:** We alternatingly compute the wanted eigenpairs of S_- and S_+ , one by one, while expanding the subspace using the residual of the currently iterated eigenpair;
3. **Sequential:** We first compute all the wanted eigenpairs of S_- , and subsequently the wanted eigenpairs of S_+ , while using the residual of the currently iterated eigenpair in the subspace expansion.

The convergence history of these three variants combining two Nonlinear Arnoldi iterations for the pair of problems S_{\pm} and of the single Nonlinear Arnoldi iteration for S_- is shown in Figure 4. The fast alternating method found a pair λ_k^- and λ_k^+ almost immediately after one another, while the slowly alternating version completed the solve for the eigenvalue λ_k^- and then with the acquired knowledge it took only a few iterations for the corresponding eigenvalue λ_k^+ . The sequential variant computed all the λ^- first and then the λ^+ , gaining less than the other two in terms of the iteration number.

Since the splitting doubles the number of confined states we have to compute, it may be necessary to restart the iteration to keep the time for a solve of the projected problem moderate. We incorporated the restart schema described in [28] in all the variants. We restarted the methods whenever the dimension of the search subspace excluding the eigenvectors exceeded a prescribed threshold and the computation of a pair λ_k^{\pm} was completed. In the sequential variant we also independently restarted, after all λ^- or λ^+ , respectively, have been computed. In all cases after restart we kept three more vectors per problem (σ_z, ℓ) than eigenvectors computed so far.

From the convergence plots we learn that the overall number of iterations per four pairs $\lambda_k^{\pm}, k = 1, \dots, 4$ is comparable for the first two variants, while the third variant needs in either case more iterations. However, in terms of the computation time the third variant, though still slightly slower than the other two if B is small, becomes faster for large values of B . This effect gets more pronounced the more confined states are to be computed. This reflects the fact that if the eigenvectors are strongly related, we lose more throwing away a great part of the already assembled search subspace than when their relation is weaker, in which case we gain more by solving smaller, due to the subspace size reduction, projected problems.

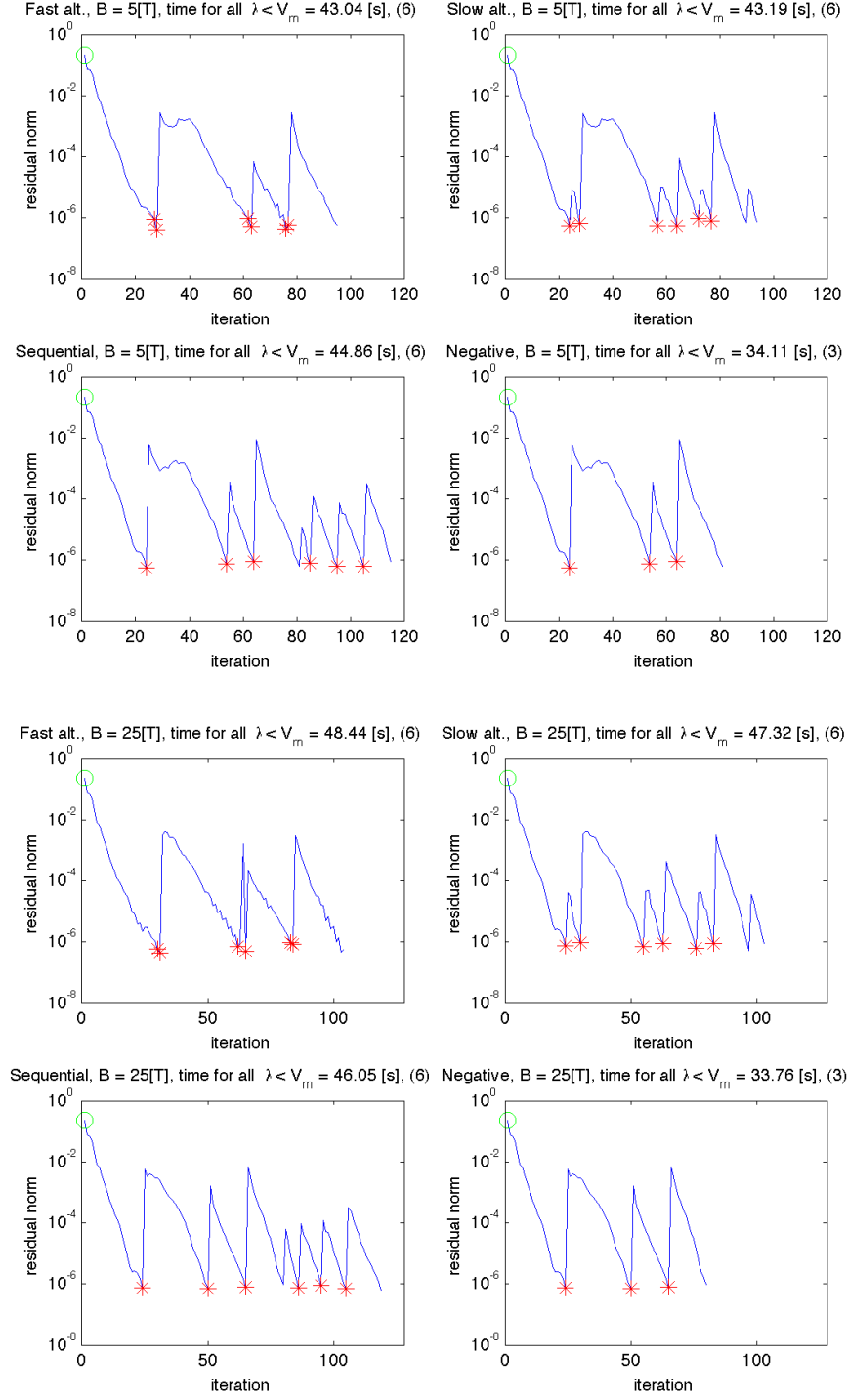


Figure 4: Convergence of all three variants of our method for the pair of problems S_{\pm} , (1-3,5-7) and of the Nonlinear Arnoldi method for S_- (4,8), for $B = 5[T]$ and $B = 25[T]$, respectively.

Table 4 displays the CPU times required by the Nonlinear Arnoldi method for computing the first four eigenpairs of S_- and by the second variant of our method for the first four pairs λ_k^\pm of S_\pm for different magnetic fields. The computation times per eigenvalue are given for $B = 25[\text{T}]$ in Table 5. For all the methods we used the incomplete LU decomposition with the threshold 10^{-2} of $S(0.1)$, i.e. problem without the magnetic field, $B = 0$, as the preconditioner, which proved the most cost efficient from the different preconditioning strategies we tested. We did not update the preconditioner during the iteration. The subspace size threshold triggering the restart was set to 200 and was not exceeded by any method, thus except for the third variant no restarts happened.

Table 4: Computation time for the Nonlinear Arnoldi method applied to compute 4 smallest eigenvalues of S_- and the second variant of our method applied to the pair S_\pm .

B [T]	total time (N.Arn. S_-) [s]	#iter	total time (2nd v. S_\pm) [s]	#iter
1	45.58	80	51.64	86
5	47.22	81	57.32	94
10	47.29	83	61.86	98
15	52.13	88	68.82	104
20	47.96	81	71.14	104
25	45.24	80	72.4	106

Table 5: Computation times per eigenvalue for the Nonlinear Arnoldi method applied to S_- and the second variant of our method applied to the pair S_\pm for $B = 25[\text{T}]$.

\pm	λ	time (N.Arn.) [s]	time (2nd v. S_\pm) [s]
+	0.2394	-	11.17
-	0.2411	11.1500	2.79
+	0.3378	-	13.94
-	0.3387	13.22	5.27
+	0.3767	-	10.63
-	0.3774	9.39	6.04
+	0.4169	-	15.38
-	0.4171	11.48	7.18

The deformation and splitting of the energy levels of the pyramidal quantum dot in dependence of the value of the magnetic field strength B is shown in Figure 5.

7.2 Quantum ring

Our second example is an elliptical quantum ring obtained by a revolution around the z -axis of an ellipse with the principal axes $a = 10\text{nm}$ (along the r -

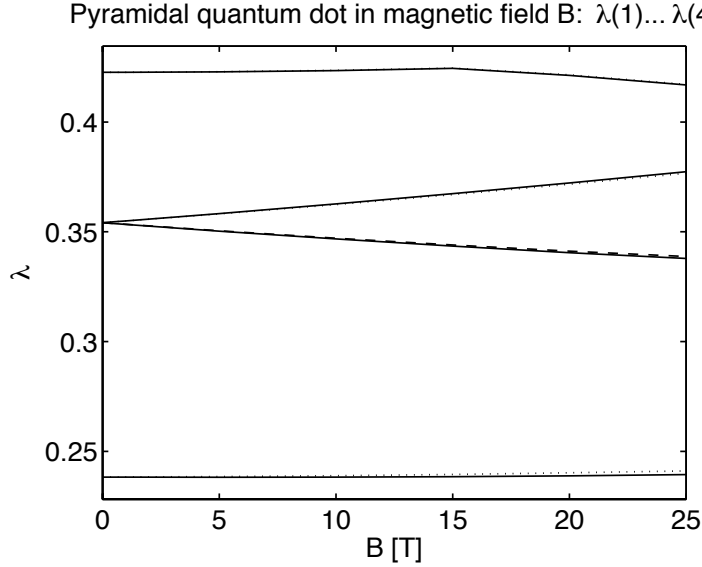


Figure 5: Splitting of the energy levels of the pyramidal quantum dot in dependence of the magnetic field strength B .

axis) and $b = 2.4\text{nm}$ (along z -axis), centred at $(r_0, z_0) = (20, 0)\text{nm}$, embedded in a cylindrical matrix of radius 40nm and height 10nm . As in the previous example we expose the ring to the magnetic field of strengths $B = 1, 5, 10, 15, 20, 25[\text{T}]$ directed along the z -axis.

We discretized the resulting sequence of two dimensional problems (13) on a triangular grid with quadratic Lagrange elements. To guarantee the convergence of the Nonlinear Arnoldi method for the problems (22) we check the discrete versions of conditions (17) and (18) for all required values of $|\ell|$, here we assume $|\ell| = 0, 1, 2, 3$. The discrete version of the eigenvalue problem (16) is of the same type as (23) with the difference, that the matrix K depend on B and $|\ell|$ and M is different for $\ell = 0$ and $\ell \neq 0$ due to the different boundary conditions on the rotational axis. The smallest eigenvalue of the discrete version of (16) for different $|\ell|$ and B values are displayed in Table 6.

The condition (17) holds if

$$\kappa_{min} > \frac{\max\{\omega_q^B(\lambda), \omega_m^B(\lambda)\}}{\min\left\{\frac{\hbar^2}{2m_q(\lambda)}, \frac{\hbar^2}{2m_m(\lambda)}\right\}} \quad \text{for every } \lambda \in J. \quad (26)$$

It can be further simplified by employing the knowledge about the functions $\omega_j^B(\lambda)$. Arguing similarly as in the previous example we have

$$\max\{\omega_q^B(\lambda), \omega_m^B(\lambda)\} = \omega_q^B(\lambda),$$

which is monotonic. We bound the right hand side by its maximum. Again, it is

Table 6: Smallest eigenvalue of discrete version of (16) for $|\ell| = 0, 1, 2, 3$ and $B = 1, 5, 10, 15, 20, 25[\text{T}]$.

$ \ell \backslash B [\text{T}]$	1	5	10	15	20	25
0	0.1025	0.1065	0.1139	0.1215	0.1291	0.1367
1	0.1082	0.1148	0.1291	0.1443	0.1595	0.1747
2	0.1156	0.1240	0.1444	0.1671	0.1898	0.2126
3	0.1246	0.1344	0.1598	0.1899	0.2202	0.2506

possible for each $|\ell|$ to factor out B . Thus we arrive at the following inequality

$$\frac{\kappa_{min}}{B} > \max_{\lambda \in J} \frac{\frac{1}{2}\mu_B |g_q(\lambda)| + |\ell| \frac{e\hbar}{2m_q(\lambda)}}{\min \left\{ \frac{\hbar^2}{2m_q(\lambda)}, \frac{\hbar^2}{2m_m(\lambda)} \right\}}, \quad (27)$$

where κ_{min} depends on $|\ell|$ and B while the right hand side depends only on $|\ell|$. As we gather from Table 6 κ_{min} grows slower than B therefore the critical condition to check is the largest B of interest. However, it is necessary to check the condition for each $|\ell|$ separately. Table 7 gives the values of $\kappa_{min}/25[\text{T}]$ and the right hand side for $|\ell| = 0, 1, 2, 3$.

 Table 7: Left and right hand sides of condition (27) for $B = 25\text{T}$.

$ \ell $	0	1	2	3
κ_{min}/B	0.0055	0.0070	0.0085	0.0100
r.h.s.	0.0004	0.0027	0.0050	0.0073

The second condition (18) is verified by the similar argument as in the last example. Here we check whether

$$\max \left\{ \eta_q^{B'}(\lambda), \eta_m^{B'}(\lambda) \right\} \leq 1.$$

As before, it is possible to single out the dependence on B . Since $\eta_j^{B'}(\lambda)$ are monotonically falling functions and their dependence on $|\ell|$ can be bounded by the maximal value of $|\ell|$, $|\ell| = 3$ in our case, we have

$$\max_{\lambda \in J} \left\{ \eta_q^{B'}(\lambda), \eta_m^{B'}(\lambda) \right\} = \max \left\{ \eta_q^{B'}(0), \eta_m^{B'}(0) \right\} \approx 0.1805 \cdot 10^{-1} B$$

from which we follow that the condition (18) is satisfied for all $B \leq 55[\text{T}]$.

We learned from the previous example that the eigenfunctions corresponding to the splitted energy levels are correlated. We expect the same in the axially symmetric case. However, for the latter we encounter a fourfold if $\ell \neq 0$ and

twofold splitting otherwise. Both the terms responsible for splitting in (15) are weighted with the bilinear forms $b_j(\cdot, \cdot)$ which again supports our belief.

To prove we are right we conducted a similar experiment in for the last section. We computed the singular value decomposition of the matrix assembling three eigenvectors corresponding to three leading eigenvalues of each of the problems (σ_z, ℓ) , $\ell = \pm 1, \sigma_z = \pm 1, [X_-, X_+, X_-, X_+]$.

The singular values are listed in Table 8. We observe the gaps of order

Table 8: Singular values of $[X_-, X_+, X_-, X_+]$ for $|\ell| = 1$.

$B[\text{T}] \backslash \sigma$	σ_1	σ_2	σ_3	σ_4	σ_5	σ_6	σ_7	σ_8	σ_9	σ_{10}
5	2.4	1.8	1.7	2.9e-3	2.2e-3	2.0e-3	4.7e-5	3.5e-5	2.9e-5	9.1e-7
25	2.5	1.8	1.6	1.4e-2	7.5e-3	6.2e-3	2.0e-4	1.3e-4	1.1e-4	5.2e-6

$\approx 10^{-2}$ between each three singular values, which is an indicator of a strong overlap of the eigensubspace of all four problems.

Therefore, it is beneficial to carry out all four iterations simultaneously and let them use the same search subspace. For combining the four iterations we used strategies analogous to those in the last example, with the difference, that we alternated between four problems in first two cases, while in the third variant we compute all the wanted eigenvalues of each of the four problems one after another. As in the last example to prevent the unlimited search subspace growth, we restarted the first two variants whenever the dimension of the search subspace excluding eigenvectors exceeded the prescribed threshold and the quadruple had been completed, while in the third variant we restarted also when we completed the computation of all wanted eigenpairs of one of the four problems. In all cases after a restart we kept only the eigensubspace and three additional vectors for each problem. Since the plane problems are real and have in general less degrees of freedom than the three dimensional problem, the preconditioner (here incomplete LU with threshold 10^{-2}) can be computed at low cost, so we do not experiment with its recycling. Moreover, we allow the first two variants to compute a new preconditioner, whenever the convergence speed becomes to slow.

Figure 6 shows the convergence of the three variants of our method applied to S_{\pm} and of the Nonlinear Arnoldi method applied to S_- for $|\ell| = 1$ and $B = 5[\text{T}]$ and $B = 25[\text{T}]$, respectively. Again the most robust variant is the second one, which is the fastest for both the weak and strong magnetic fields. Though, the iteration numbers for the first two variants are comparable the CPU time needed by the first variant is much longer, which is due to the expensive incessant switching between the four problems. Again, we observe that the third variant improves with the growing magnetic field, for the same reason as in our first example. The comparison of the second variant of our method and the Nonlinear Arnoldi method in terms of the computation time and the number of iterations is shown in Table 9. For the weak magnetic field, $B = 5[\text{T}]$, the gain is about 40% of the CPU time and 65% of the iterations, while for the strong field, $B = 25[\text{T}]$, it decreases to 25% and 50%, respectively.

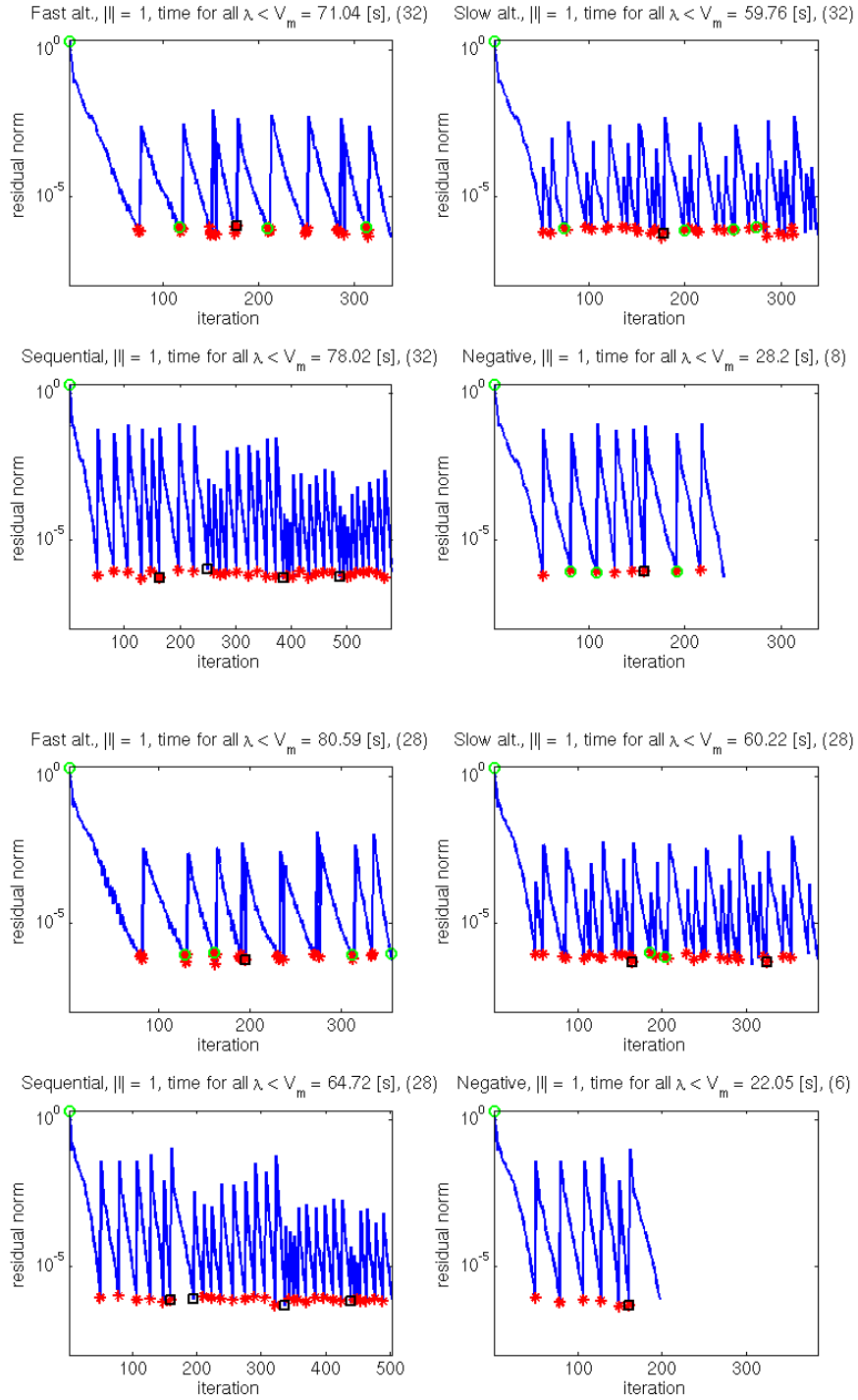


Figure 6: Convergence of all three variants of our method for the quadruple of problems S_{\pm}^{ℓ} , $|\ell| = 1$ (1–3,5–7) and of the Nonlinear Arnoldi method for S_{-}^{ℓ} , $\ell = 1$ (4,8) for $B = 5$ [T] and $B = 25$ [T], respectively. The squares designate the restarts.

Table 9: Time and iteration number for computation of the confined states by Nonlinear Arnoldi applied to S_-^ℓ for $\ell = 1$ and the second variant of our method (Quadruple Simult.N.Arn) applied to S_\pm^ℓ for $|\ell| = 1$, for $B = 5, 15, 25$ [T].

B [T]	N.Arn. CPU [s]	# iter	QS.N.Arn. CPU [s]	# iter
5	32.2	240	76.7	338
15	32.0	240	91.9	362
25	25.4	197	78.0	384

Figure 7 shows the splitting and deformation of the first six energy levels (enumeration w.r.t. problem with $B = 0$) in dependence of the magnetic field strength. The effect is much stronger than in the case of the dot, because the ring shape is more prone to trap the perpendicular magnetic field. This results in a periodic oscillations of the electronic levels, see also e.g. [11].

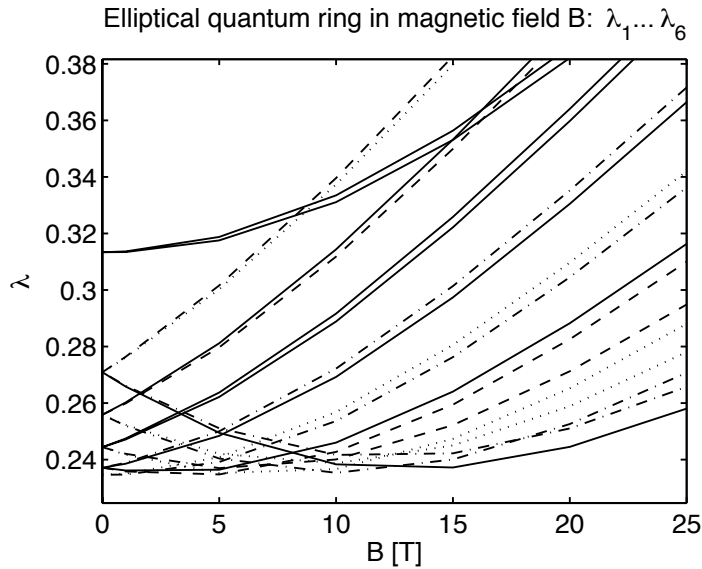


Figure 7: Splitting and deformation of the energy levels of the elliptic quantum ring in dependence of the magnetic field B .

Though in our simulations we have restricted ourselves to the Nonlinear Arnoldi method we could as well have used the Jacobi Davison iteration or even combine the two methods. However, our numerical experience is that if the problem size allows for a good quality preconditioner, as it was the case in our examples, the Nonlinear Arnoldi method works better. Nevertheless Jacobi Davidson could be the method of choice if the sizes of the eigenvalue problems were much larger.

8 Conclusions

In the framework of one-band nonparabolic effective Hamiltonian in the homogenous magnetic field we derived a pair/quadruple of the nonlinear eigenvalue problems corresponding to different spin orientations and in the case of the rotational symmetry also to $\pm\ell$ quantum number. To the best of our knowledge there is no simulation of truly three dimensional structures like the pyramid in the magnetic field in a nonparabolic regime. We derived conditions for both the three dimensional problem as for the plane problems (resulting from the separation of the axial direction) to allow the minmax characterization of their relevant eigenvalues (confined states). These conditions hold for both our examples of the pyramidal quantum dot and the quantum ring and the common InAs/GaAs heterojunction. In our approach the problems were discretized with Galerkin methods, yielding large and sparse rational matrix eigenvalue problems requiring numerical treatment with iterative projection methods. Endowed with the minmax principle the iterative methods like Nonlinear Arnodi can effectively prevent the repeated convergence to the already computed eigenpairs. For both cases we devised specially tailored iterative methods simultaneously handling the pair/quadruple of the problems and thereby saving about up to 40% of the overall computation time.

Acknowledgement

The authors thank Oleksandr Voskoboynikov for his comments on the physical relevance of the model under consideration.

References

- [1] G. Arioli and A. Szulkin. A semilinear Schrödinger equation in the presence of a magnetic field. *Arch. Rational Mech. Anal.*, 170:277–295, 2003.
- [2] I. Babuska and J. Osborn. Eigenvalue problems. In P.G. Ciarlet and J.L. Lions, editors, *Handbook of Numerical Analysis*, volume II, pages 641–923. North Holland, Amsterdam, 1991.
- [3] G. Bastard. *Wave Mechanics Applied to Semiconductor Heterostructures*. Les editions de physique, Les Ulis Cedex, 1988.
- [4] M. Betcke. *Iterative Projection Methods for Nonlinear Eigenvalue Problems with Applications*. Dissertation.de, 2007. PhD Thesis, Hamburg University of Technology.
- [5] M. M. Betcke and H. Voss. Stationary schrödinger equations governing electronic states of quantum dots in the presence of spin-orbit splitting. *Applications of Mathematics*, 52(3):267–284, 2007.

- [6] M. M. Betcke and H. Voss. Numerical simulation of electronic properties of coupled quantum dots on wetting layers. *Nanotechnology*, 19(16):165204 (10pp), 2008.
- [7] T. Betcke and H. Voss. A Jacobi–Davidson–type projection method for nonlinear eigenvalue problems. *Future Generation Computer Systems*, 20(3):363 – 372, 2004.
- [8] S. L. Chuang. *Physics of Optoelectronic Devices*. John Wiley & Sons, New York, 1995.
- [9] M. J. Estaban and P.-L. Lions. *Partial Differential Equations and the Calculus of Variations*, volume 1, chapter Stationary solutions of nonlinear Schrödinger equations with an external magnetic field. Birkhäuser, Berlin, 1989.
- [10] FEMLAB, Version 3.1. COMSOL, Inc., Burlington, MA, USA, 2004.
- [11] B. C. Lee, O. Voskoboynikov, and C. P. Lee. III–IV semiconductor nanorings. *Physica E*, 24:87–91, 2004.
- [12] Y. Li. Numerical calculation of electronic structure for three-dimensional nanoscale semiconductor quantum dots and rings. *J. Comput. Electronics*, 2:49 – 57, 2003.
- [13] Y. Li, H.-M. Lu, O. Voskoboynikov, C.P. Lee, and S.M. Sze. Dependence of energy gap on magnetic fields in semiconductor nano-scale quantum rings. *Surface Science*, 532–535:811 – 815, 2003.
- [14] Y. Li, O. Voskoboynikov, C. P. Lee, S. M. Sze, and O. Tretyak. Effect of shape and size on electron transition energies of InAs semiconductor quantum dots. *Jpn.J.Appl.Phys.*, 41:2698 – 2700, 2002.
- [15] E. H. Lieb and M. Loss. *Analysis*. American Mathematical Society, 2001.
- [16] M. Markiewicz and H. Voss. A local restart procedure for iterative projection methods for nonlinear symmetric eigenproblems. In A. Handlovicova, Z. Kriva, K. Mikula, and D. Sevcovic, editors, *Algoritmy 2005, 17th Conference on Scientific Computing, Vysoke Tatry - Podbanske, Slovakia 2005*, pages 212 – 221, Bratislava, Slovakia, 2005. Slovak University of Technology.
- [17] M. Markiewicz and H. Voss. Electronic states in three dimensional quantum dot/wetting layer structures. In M. Gavrilova et al. (eds.), editor, *Proceedings of ICCSA 2006*, volume 3980 of *Lecture Notes on Computer Science*, pages 684 – 693, Berlin, 2006. Springer Verlag.
- [18] K. Meerbergen. Locking and restarting quadratic eigenvalue solvers. *SIAM J. Sci. Comput.*, 22(5):1814–1839, 2000.

- [19] K. Meerbergen. The quadratic arnoldi method for the solution of the quadratic eigenvalue problem. *SIAM Journal on Matrix Analysis and Applications*, 30(4):1463–1482, 2008.
- [20] A. Neumaier. Residual inverse iteration for the nonlinear eigenvalue problem. *SIAM J. Numer. Anal.*, 22:914 – 923, 1985.
- [21] B. Opic and A. Kufner. *Hardy-type inequalities*. Longman Scientific & Technical, Essex, England, 1990.
- [22] A. A. Sirenko, T. Ruf, N. N. Ledentsov, A. Yu. Egorov, P. S. Kop’ev, V. M. Ustinov, and A. E. Zhukov. Resonant spin-flip Raman scattering and localized exciton luminescence in submonolayer InAs-GaAs structures. *Solid State Comm.*, 97, 1996.
- [23] G. L. Sleijpen, G. L. Booten, D. R. Fokkema, and H. A. van der Vorst. Jacobi-Davidson type methods for generalized eigenproblems and polynomial eigenproblems. *BIT*, 36:595 – 633, 1996.
- [24] O. Voskoboynikov, Y. Li, H.-M. Lu, C.-F. Shih, and C. P. Lee. Energy states and magnetization in nanoscale quantum rings. *Phys.Rev B*, 66:155306–1 – 155306–6, 2002.
- [25] O. Voskoboynikov, C. M. J. Wijers, J. L. Liu, and C. P. Lee. Magneto-optical response of layers of semiconductor quantum dots and rings. *Phys.Rev B*, 71:245332–1 – 245332–12, 2005.
- [26] H. Voss. An Arnoldi method for nonlinear symmetric eigenvalue problems. In *Online Proceedings of the SIAM Conference on Applied Linear Algebra, Williamsburg.*, <http://www.siam.org/meetings/laa03/>, 2003.
- [27] H. Voss. Initializing iterative projection methods for rational symmetric eigenproblems. In *Online Proceedings of the Dagstuhl Seminar Theoretical and Computational Aspects of Matrix Algorithms, Schloss Dagstuhl 2003*, <ftp://ftp.dagstuhl.de/pub/Proceedings/03/03421/03421.VoszHeinrich.Other.pdf>, 2003.
- [28] H. Voss. An Arnoldi method for nonlinear eigenvalue problems. *BIT Numerical Mathematics*, 44:387 – 401, 2004.
- [29] H. Voss. A rational eigenvalue problem governing relevant energy states of a quantum dots. *J. Comput. Phys.*, 217:824 – 833, 2006.
- [30] H. Voss and B. Werner. A minimax principle for nonlinear eigenvalue problems with applications to nonoverdamped systems. *Math. Meth. Appl. Sci.*, 4:415–424, 1982.